An open source tool for reliability evaluation of distribution systems with renewable generators

S. Conti, S.A. Rizzo
Department of Electrical, Electronics and Computer Engineering, University of Catania, Italy
stefania.conti@dieei.unict.it (0000-0002-4646-595X) santi.rizzo@dieei.unict.it (0000-0001-5924-8105)

***Abstract*—**Future smart electrical distribution systems could adopt switch remote control and advanced automation systems to operate in autonomous mode (islanding) some portions of the network in order to improve system reliability. In this perspective, a free code able to assess distribution reliability by using analytical or Monte Carlo simulation methods accounting for intentional islanding operation is presented. An effective network representation and data structure, which have led up to the implementation of two automatic and general procedures, are proposed. The procedures share common underlying information in order to speed up calculation. A further merit of the tool is that it enables the user to quickly and simply create the input files. The reliability indices of three distribution networks have been computed by means of the developed software for different scenarios, that is when island mode of operation is not permitted by regulation, and when island mode is permitted (intentional islanding) with the local load either partially or totally supplied by renewable distributed generators. The free code, the input files and the results related to the considered networks are available online at: http://www.dieei.unict.it/users/sconti/psrs.htm.

Keywords*—Renewable distributed generation; distribution system reliability; open source software; microgrids; power system simulation; smart grids.*

NOMENCLATURE

CAIDI	customer average interruption duration index
CBS	circuit breaker + sectionalizer
DG	distributed generator
EDN	electrical distribution network
LP	load point
MCS	Monte Carlo simulation (RMCS Random MCS - SMCS Random MCS)
MTBF	mean time between failures
MTTF	mean time to failure
MTTR	mean time to repair
MV	medium voltage
NB	number of branches
PoA	Probability of adequacy
PS	primary substation
SB	source branch
SN	source node
SAIDI	system average interruption duration index
SAIFI	system average interruption frequency index
SOB	set of branches (they are the brances in a segment)
SON	set of nodes (they are the nodes in a segment)
f	branch failure frequency
N_C	number of customers
t_{AV}	time to be available (it is the time to reconnect the DG units disconnected due to a fault in the network)
t_R	branch repair time (set to MTTR)
t_S	sectionalizer switching time

I. INTRODUCTION

Reliability assessment of electrical distribution network (EDN) in presence of renewable distributed generators (DGs) is a crucial point for the distribution network operator (DNO). Usually, Monte Carlo simulation (MCS) or analytical methods are used to assess EDN reliability [1]-[10]. Actually, such methods give an estimation of some reliability indices by exploiting historical data of network components, faults and load profiles [10]. These methods do not consider the presence of DGs or the possibility to intentionally operate some portions of the EDN in island mode (i.e. temporary autonomous microgrids) after a fault occurs [11]. Moreover, their application in general networks asks for: on one hand, general representation of network data (topology, load and so on); on the other hand, algorithms and routines able to manipulate the data in accordance with the calculation method as well as to implement their calculation procedures. In this perspective, many algorithms have been proposed to evaluate EDN reliability in general networks [12]-[19].

In the last years, the growing presence of renewable DGs has made indispensable the development of new MCS and analytical methods able to account for the potential benefits deriving from intentional islanding [20]-[22]. In [23] a method for reliability evaluation in active EDNs with multiple microgrids based on a MCS is proposed. In [24] the reliability assessment problem in active EDNs with low and high DG penetration level by using the MCS method is treated. The sequential MCS adopted in [25] incorporates customer satisfaction constraints, thus enabling reliability evaluation under optimal network operation. In [26] sequential MCS is applied to estimate the impact of the islanded operation of a microgrid on the load point (LP) and system indices related to yearly frequency and duration of interruptions. A reliability evaluation MCS method is proposed in [27] based on direct cyber-power interdependencies. An analytical framework has been devised in [28] to evaluate the reliability considering the uncertain nature of wind turbines output generation, the variations in stored energy of electric vehicles along with the fluctuations of load profiles. A Markov model that evaluates the reliability of a future EDN including conventional or renewable DG units is presented in [29]. DGs and electric vehicles' batteries as well as Markov models are also been considered in [30]. An analytical method based on segmentation which uses two matrices for evaluating EDN reliability in presence of DGs is described in [31].

Therefore, although new MCS and analytical methods which account for islanding have been proposed, new algorithms and software able in integrating these methods are

necessary, as the previous ones [12]-[19] were developed for old methods that neglect islanding. In this perspective, this paper describes the core procedures of a free code developed on the ground of MCS and analytical methods proposed by the authors in [32] and [33], respectively, which consider the effect of islanding on EDN reliability. These methods exploit segmentation to quickly evaluate reliability with the advantage of using only one matrix [33]. More specifically, the nodes (MV buses or switching substations) and the branches (electrical equipment between two nodes) in a segment are grouped, respectively, in a set of nodes (SON) and in a set of branches (SOB). A procedure identifies the SOBs and SONs, while the other identifies, for each couple SOB-SON, the topological *case* (defined by the reciprocal position of LP, fault, circuit breakers and sectionalizers) to be considered as described in [33]. The identification of the SOBs, SONs and topological cases is necessary to quickly evaluate the reliability of any radial EDN. The present paper also proposes a network representation and data structure to be exploited effectively by the implementation of the two aforementioned procedures. Such procedures share common underlying information related to the network in order to speed up the reliability analysis.

In the last years, new simulation tools for designing, planning, controlling, managing and operating EDNs have been developed to face the new challenges of smart grids [34]-[38]. In view of planning the future smart grid, the development of the source code, available online [39] for free under the GNU General Public License, allows researchers and practitioners to further improve the results accuracy of the reliability analysis methods implemented in the code by also integrating new features too (e.g. power flow analysis [40], stability analysis [41] and so on), as well as to properly combine the software with optimization methods [42]-[44], and so on.

The paper is structured as follows. In section II the adopted network representation is described. In section III and IV, the implemented procedures are presented. The considered analytical formulation and MCS involve the adequacy calculation of conventional and renewable DGs supplying autonomous microgrids [45]-[51] by using probabilistic models. Some methods and new general analytical expressions to evaluate local generators adequacy, accounting for load shedding (user load disconnection) and curtailment (user load reduction), have been presented in [33], [52], [53]. Such a quantity has been evaluated through a "Probability of Adequacy" (PoA), which is provided as input to the software. Finally, in section V a case study is presented to show the simplicity of the input files and the code ability to correctly identify SOB, SON and topological case. Moreover, the reliability indices have been computed in various scenarios. The worst and best ones have been simulated with DIgSILENT Power Factory to validate the results obtained by the proposed tool.

II. Network Representation

The considered network representation is based on the concept of line as a generalization of backbone and lateral. In particular, when the "lateral line" *x* of the backbone has some lines connected to it, these lines are considered as its laterals and then *x* is their "backbone line". The lines are sequentially numbered by considering firstly the main backbone (line level 0) and then its laterals (line level 1) starting from the lateral connected to the node closest to the primary substation (PS), and so on. Then, each lateral with some lines connected to it is in turn considered as a backbone (line level 1) and the lines become its laterals (line level 2). The previous numbering procedure is applied to the lines of level 2, and so on.

The branches of each line are sequentially numbered starting from the one closest to the PS. The nodes take the number of the upstream (with reference to PS position) branch.

Fig.1 shows an example of a generic radial EDN (A), two of its possible network representations (B, C) based on the described network representation and numbering procedure, and the numeration correspondence among the three representations. Therefore, any radial network can be represented as a set of lines and the essential information about a line is: the line number (i.e. its *id*), the *id* of the node (called source node, SN) where the line is connected, the number of branches (NB) in the line and the *id* of the first branch (called source branch, SB). The last piece of information is necessary to distinguish among different lines connected to the same node. Table 1 reports such information for the network in Fig.1C. Note that the PS is considered as node 0. Actually, the information in the first column can be neglected by assuming the lines in ascending order.

The elements in the diagonal of the branch-node incidence matrix are equal to 1 when the aforesaid nodes numeration is adopted. Table 2 reports the position of the other non-zero elements (they are equal to -1) for the network in Fig.1C. Therefore, the size of branch-node incidence matrix increases with the number of branches (it is twice as much the number of branches) while the adopted one with the number of lines.

TABLE 1
TOPOLOGY DESCRIPTION OF THE NETWORK IN FIG.1C.
THE LINE ID CAN BE NEGLECTED WHEN THE LINES ARE IN ASCENDING ORDER.

Line ID	SN	SB	NB
1	0	1	8
2	2	9	5
3	2	14	3
4	2	17	8
5	3	25	3
6	5	28	5
7	5	33	3
8	6	36	9
9	11	45	2
10	22	47	2
11	31	49	2
12	40	51	2
13	40	53	3
14	43	56	1
15	47	57	2
16	51	59	2
17	54	61	3
18	54	64	3

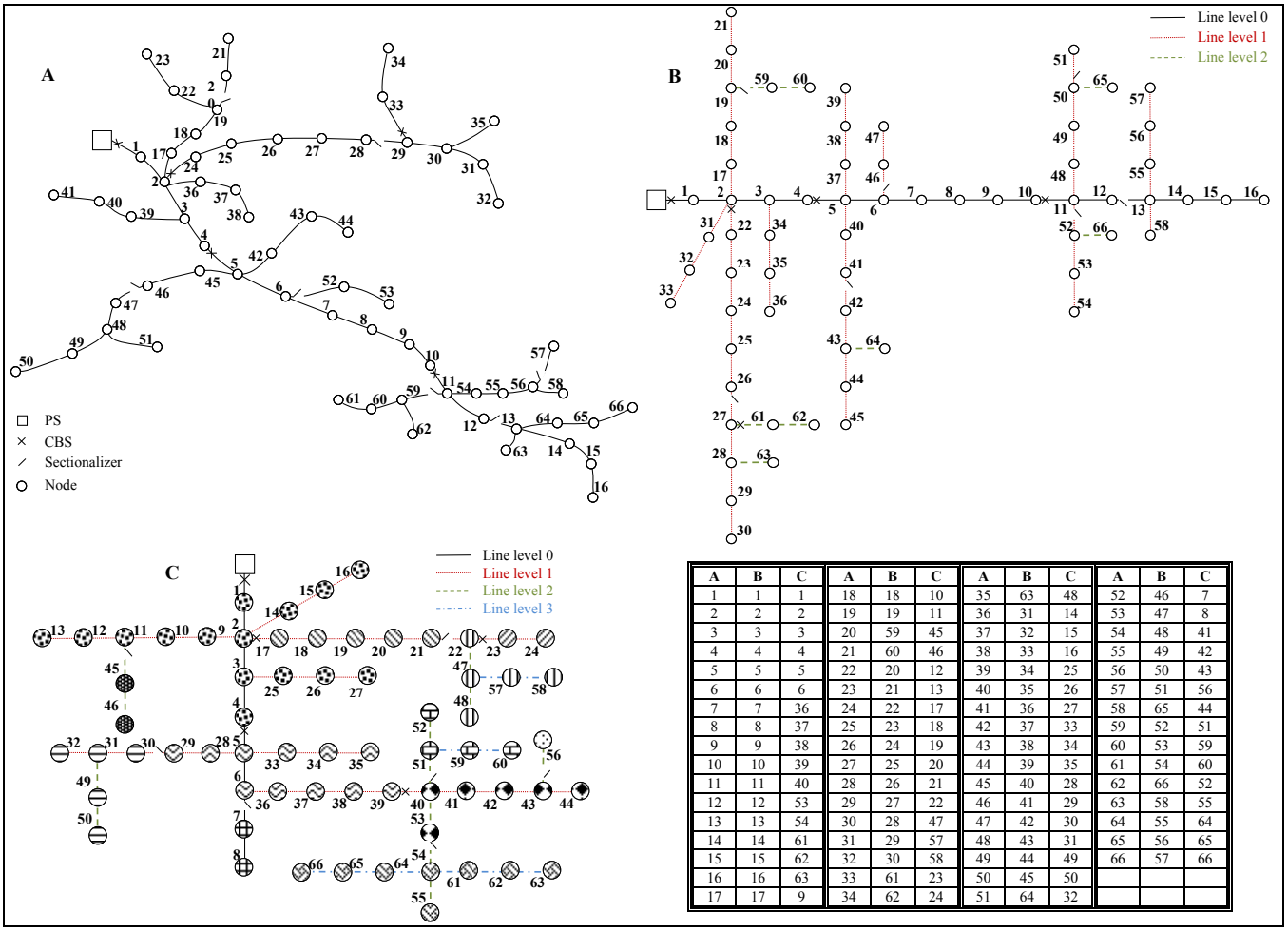

A	B	C	A	B	C	A	B	C	A	B	C
1	1	1	18	18	10	35	63	48	52	46	7
2	2	2	19	19	11	36	31	14	53	47	8
3	3	3	20	59	45	37	32	15	54	48	41
4	4	4	21	60	46	38	33	16	55	49	42
5	5	5	22	20	12	39	34	25	56	50	43
6	6	6	23	21	13	40	35	26	57	51	56
7	7	36	24	22	17	41	36	27	58	65	44
8	8	37	25	23	18	42	37	33	59	52	51
9	9	38	26	24	19	43	38	34	60	53	59
10	10	39	27	25	20	44	39	35	61	54	60
11	11	40	28	26	21	45	40	28	62	66	52
12	12	53	29	27	22	46	41	29	63	58	55
13	13	54	30	28	47	47	42	30	64	55	64
14	14	61	31	29	57	48	43	31	65	56	65
15	15	62	32	30	58	49	44	49	66	57	66
16	16	63	33	61	23	50	45	50			
17	17	9	34	62	24	51	64	32			

Fig. 1. An example of radial EDN and its representation. The nodes of each SON in figure C are marked with the same symbol.

TABLE 2
ELEMENTS EQUALS TO -1 IN THE BRANCH-NODE INCIDENCE MATRIX OF THE NETWORK IN FIG.1 C.
THE ELEMENTS IN THE DIAGONAL ARE 1, THE OTHERS ARE 0.

b-n	b-n	b-n	b-n	b-n	b-n
1-0	12-11	23-22	34-33	45-11	56-43
2-1	13-12	24-23	35-34	46-45	57-47
3-2	14-2	25-3	36-6	47-22	58-57
4-3	15-14	26-25	37-36	48-47	59-51
5-4	16-15	27-26	38-37	49-31	60-59
6-5	17-2	28-5	39-38	50-49	61-54
7-6	18-17	29-28	40-39	51-40	62-61
8-7	19-18	30-29	41-40	52-51	63-62
9-2	20-19	31-30	42-41	53-40	64-54
10-9	21-20	32-31	43-42	54-53	65-64
11-10	22-21	33-5	44-43	55-54	66-65

Compared with the branch-node incidence matrix, the proposed representation enables a more compact topology representation and the proposed procedures exploit it in order to perform their tasks more quickly. Such an advantage is more important than the information size reduction, especially for applications where many reliability computations have to be performed (e.g. when the MCS reliability tool is integrated in a multi-objective optimization tool).

The further necessary element to be provided to the tool is the number of customers connected to each node,. The information about the failure rate and repair time of each branch is provided as well. Moreover, for each switch it is necessary to indicate the type, the *id* of the installation branch, and the PoA of the potential island derived from the switch opening. Starting from the aforementioned simple information, the tool is able to rapidly compute the reliability indices related to LP and network of any radial EDN by using analytical formulation, random and sequential MCS (RMCS, SMCS), also accounting for islanding operation of temporary intentional islands supplied by the local generation.

III. SET OF BRANCHES AND SET OF NODES IDENTIFICATION

From the topological point of view, a segment *j* is the portion of the EDN located among switch *j* and the switches placed downstream from it, where "switch *j*" refers to the switch installed at branch *j*. The branches in a segment are grouped in a SOB, the nodes in a SON [33]. Segmentation enables to quickly compute EDN reliability by considering that the branches in a SOB affect a given node in the same way when a fault occurs in one of these branches. In other words, if a fault in a branch of the SOB has a given effect on a given node, a fault in another branch of the SOB produces the same effect on that node. Similarly, the nodes in a SON are affected in the same way by a given branch. In other words, if

a node of the SON is subject to a given effect by a fault in a given branch, each other node in the SON is subject to the same effect due to that fault.

Moreover, in a radial network, the number of SONs is equal to the number of SOBs and identifying the nodes belonging to a SON implies identifying the branches belonging to a SOB and vice versa. Furthermore, by the definition of "segment", it follows that the number of segments is equal to the number of switches.

The proposed strategy is based on these considerations. Therefore, in the following, a switch and the associated SOB and SON are, respectively, referred to as “related switch”, “related branch” and “related node”. Fig.2 shows the equivalent reduced network obtained when segmentation is adopted, that is SOBs and SONs are considered instead of branches and nodes.

The procedure for segments identification described below (and implemented in the software) stores some useful information, avoiding further computational effort, thanks to the network representation and data structure described before. This enables a fast identification of both segments and topological cases because this procedure finds underlying network topological information (that is the path from the PS to the "related switch" of the identified segment) which is also used by the other one (i.e. the procedure for cases identification). In figg. 3-4 the flowcharts used to find the sets (SOBs and SONs) and to compute/store the related information are reported. In particular, the path from the PS to each set is found and stored in the matrix *path* (this kind of information enables an effective cases’ identification). In the flowcharts: *rs* is the “related switch”; *ns* is the number of switches; *f*, t_R, N_c are the arrays storing respectively, the failure frequency and repair time of each branch and the number of customers of each node; similarly, *fsob*, *tsob*, *cson* store the resulting information for the SOBs and SONs; *path* is a matrix whose *rs*-th row provides the references to the switches along the path from the PS to the *rs*-th set and, *append* is a function that inserts a reference to another switch at the end of the row; *sln* is the array referring to the switch’s installation line; *flt* is the array referring to the first lateral of each line; *sb* is the array storing the *id* of the first branch for each line; *ib* is the array storing the *id* of the switches’ installation branch; *nlt* is the array storing the number of laterals of each line; *sn* and *lb* are the arrays that store, respectively, the *id* of the node where each line is connected and the *id* of the last branch of the line. Note that, the value in *f*, t_R, N_c, *sb*, *ib*, *sn* are part of the input provided to the software, as described in the previous section.

The other quantities used in the procedures are obtained by elaboration of the initial information. For the sake of brevity, the procedures adopted to this aim are not reported in the paper, even though they are implemented in the code.

Firstly, the procedure to find the segments, described in Fig.3, sets to zero the equivalent failure rate and repair time of the “related SOB”, *rs*, as well as the equivalent number of customers of “related SON” *rs*. Moreover, the *id* of the “related switch” is added to its path from the PS.

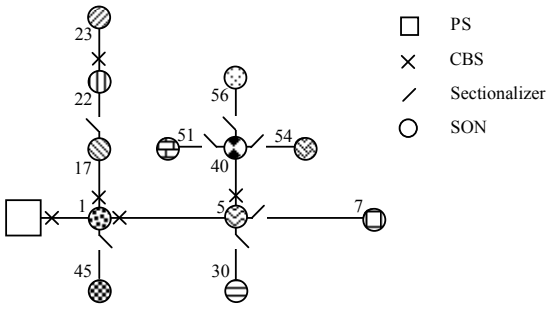

Fig. 2. EDN equivalent to the one in Fig.1C considering SOBs and SONs instead of branches and nodes.

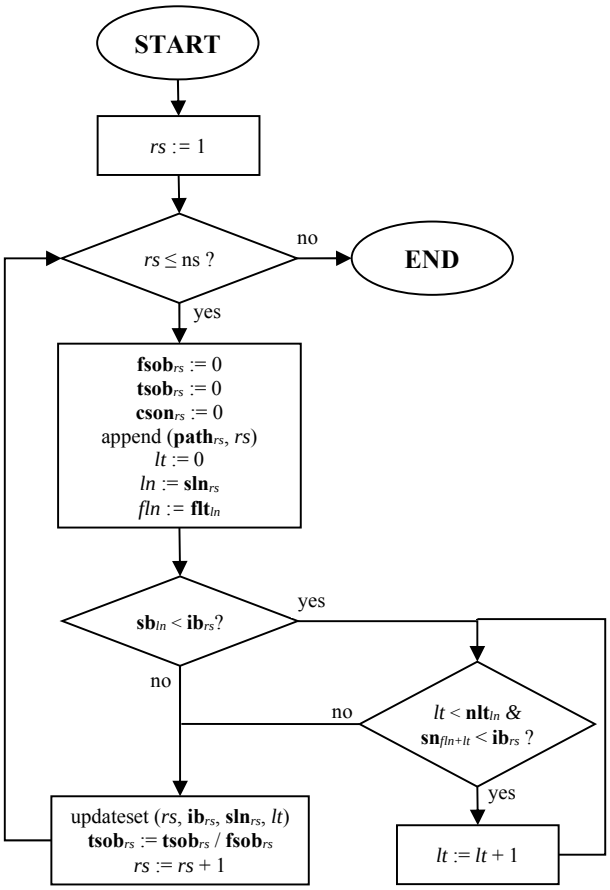

Fig. 3. Block diagram of the routine used to find the SOBs and SONs.

After that, among the laterals of the line, where the “related switch” is installed, the procedure neglects the ones upstream from the switch, that is the laterals with a source node *id* greater than the one of the installation branch of the switch (see the low-left part of Fig.3).

After that, the routine of Fig.4 is called from the one in Fig.3. If another switch, *sc* (=*rs*+1), is installed in the same line of the “related switch” and switch *sc* is located downstream from it, that is sln_{sc} is equal to *ln* (=sln_{rs}), then the installation branch of switch *sc* is a "wall", *w*, for the set.

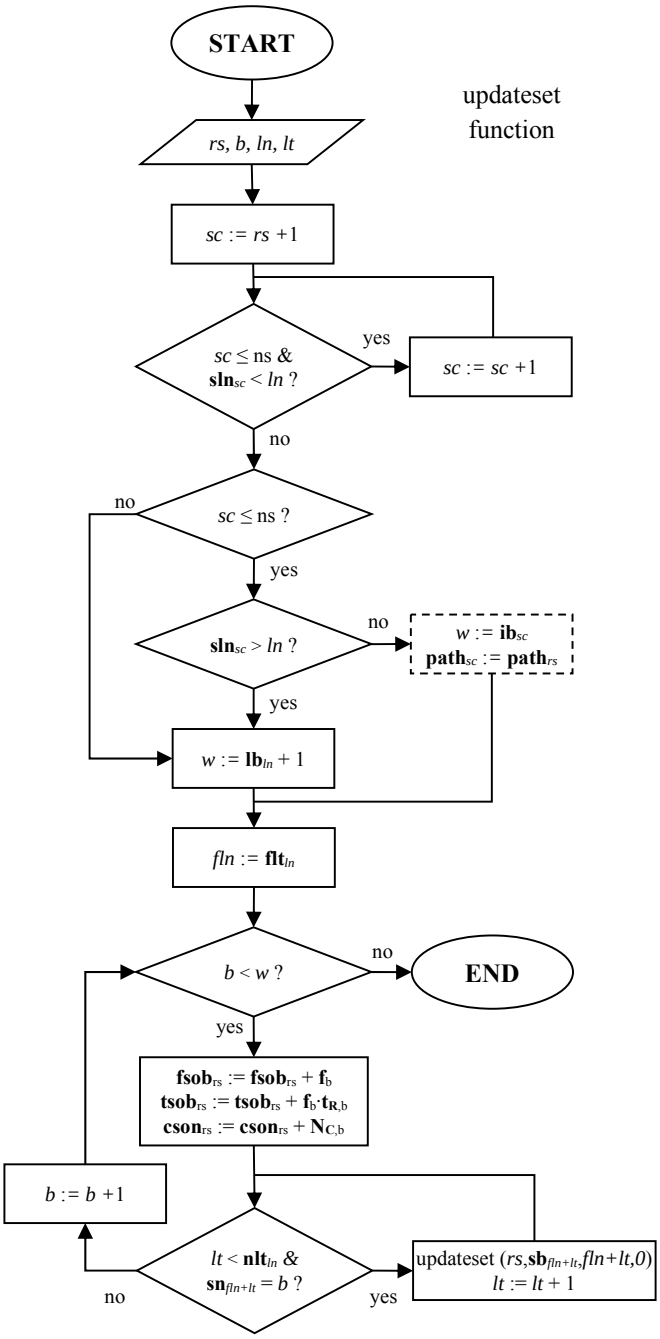

Fig. 4. Block diagram of the routine updating SOB and SON information.

The same path of the current *rs* is assigned to the current *sc*. More in general, the path assignment in Fig.4 is based on the fact that if the dashed rectangle is reached, the switch *sc* delimits the set, and then the path for this switch differs from the path of *rs* only for the reference to *sc* itself. It is worth to note that this further reference is added to the path of *sc* by using the *append* function (see Fig.3) after the aforementioned assignment. In fact, *sc* is greater than *rs* in the block diagram of Fig.4 and then, when the loop on Fig.3 sets *rs* equal to *sc*, the assignment in the dashed box is already done.

When no switch is installed downstream from the "related switch" in its same line, there is not a "wall" along the line, so a fictitious "wall" is assigned downstream from the last branch of the line, that is $w=lb_{ln}+1$ with $ln=sln_{rs}$. After that, the equivalent failure rate and repair time as well as the equivalent number of customers are cyclically updated, and the routine iteratively calls itself when a lateral is found before the "wall". Each time the routine in Fig.4 calls itself:

- *rs* does not change;
- the first branch to be considered, *b*, is the first branch of the current line (*b* is the installation branch of *rs* when this routine is called from the one in Fig.3);
- the current line in the "called" routine of Fig.4, that is *ln*, is the *lt*-th lateral in the current line of the "calling" routine in Fig.4, that is *fln*+*lt* (*ln* is the line where *rs* is installed when this routine is called from the one in Fig.3);
- the lateral in the "called" routine of Fig.4, that is *lt*, is the first lateral (when it exists) of the current line in the "called" routine of Fig.4 (*lt* is the first lateral downstream from *rs* when this routine is called from the one in Fig.3).

IV. Fast Method to Identify the Cases

In the following the topological description of each case, that is the reciprocal position combination of LP *i* (or SON *i* when segmentation is considered), faulted branch *k* (or SOB *k*) and switches is reported. A detailed description of the computational approach to be adopted in each case is reported in [32], [33]. The switches are installed at the sending end of a branch and they are sectionalizers and CBS (circuit breaker + sectionalizer installed at the same branch).

Case 1 - No switch is installed between *k* and *i*.

For example: LP *i*=42 and branch *k*=8 in Fig.1a; SON *i*=5 and SOB *k*=5 in Fig.2.

Case 2 - At least one CBS (*j*) is installed between *k* and *i*, and it is not placed between the PS and *i*.

For example: LP *i*=42, branch *k*=55, CBS *j*=11 or LP *i*=42, branch *k*=27, CBS *j*=24 in Fig.1a; SON *i*=5, SOB *k*=40, CBS *j*=40 or SON *i*=5, SOB *k*=17, CBS *j*=17 in Fig.2.

Case 3 - One or more CBSs are installed between *k* and *i* (the CBS closest to *k* is called *j*). They are all placed between the PS and *i*. Further, no sectionalizer is installed between *j* and *k*.

For example: LP *i*=42, branch *k*=40, CBS *j*=5 in Fig.1a; SON *i*=5, SOB *k*=1, CBS *j*=5 in Fig.2.

Case 3.1 - One or more CBSs are installed between *k* and *i* (the CBS closest to *k* is called *j*). They are all placed between the PS and *i*. One or more sectionalizers are installed between *j* and *k* (among those sectionalizers, the closest to *k* is called *sc*). These sectionalizers are all placed between the CBS and the PS.

For example: LP *i*=34, branch *k*=26, CBS *j*=33, sectionalizer *sc*=29 in Fig.1a; SON *i*=23, SOB *k*=17, CBS *j*=23, sectionalizer *sc*=22 in Fig.2.

Case 3.2 - One or more CBSs are installed between *k* and *i* (the CBS closest to *k* is called *j*). They are all placed between the PS and *i*. At least one sectionalizer *sc* is installed between *j* and *k*, and it is not placed between the CBS and the PS.

For example: LP *i*=42, branch *k*=21, CBS *j*=5, sectionalizer *sc*=20 in Fig.1a; SON *i*=5, SOB *k*=45, CBS *j*=5, sectionalizer *sc*=45 in Fig.2.

Case 4 - No CBS is installed between *k* and *i*, but at least one sectionalizer *j* is installed in that position, and it is not placed between the PS and *i*.
For example: LP *i*=42, branch *k*=53, sectionalizer *j*=52 in Fig.1a; SON *i*=5, SOB *k*=7, sectionalizer *j*=7, in Fig.2.
Case 5 - No CBS is installed between *k* and *i*, but one or more sectionalizers are installed in that position (the sectionalizer closest to *k* is called *j*) and they are all placed between the PS and *i.*
For example: LP *i*=31, branch *k*=26, sectionalizer *j*=29 in Fig.1a; SON *i*=22, SOB *k*=17, sectionalizer *j*=22, in Fig.2.

The use of SONs and SOBs instead of LPs and branches entails that a switch is installed in each branch of the equivalent reduced network (see Fig.2) and then, for a given SOB *k* and SON *i* (*i*≠*k*), the SOB can be located:

A. downstream from the SON;
B. upstream from the SON;
C. otherwise.

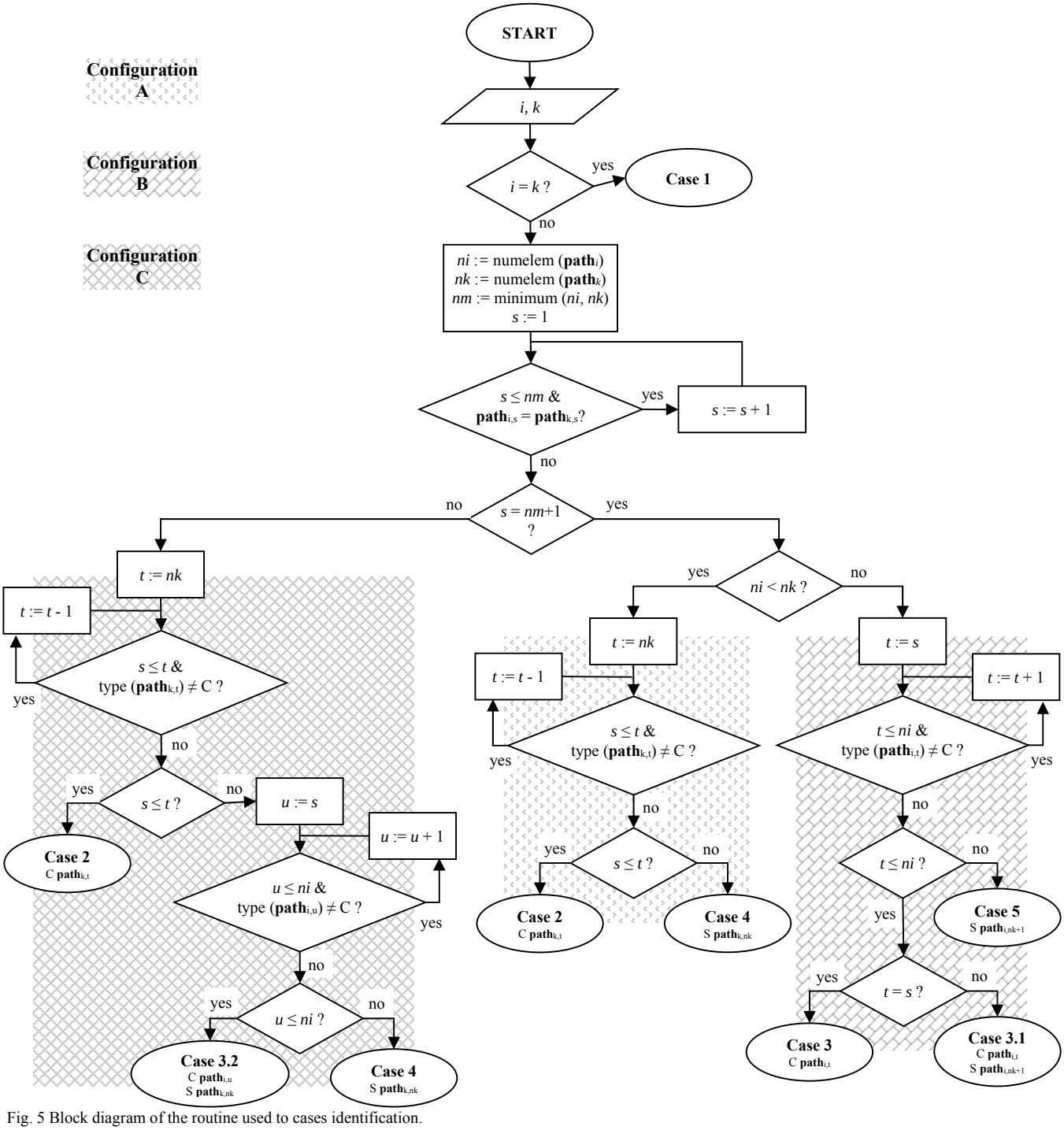

Fig. 5 Block diagram of the routine used to cases identification.

The cases identification method based on the three configurations listed before is combined with the information carried out at the identification stage of SOB/SON, that is the (underling common) information stored in *path*, to effectively identify the cases and the operating switches to be considered in the analytical formulation and MCS. Fig.5 shows the resulting computer-implementable flowchart, where: *ni* and *nk* are the number of switches installed along the path from the PS to, respectively, SON *i* and SOB *k*; *type* (*x*) returns '*C*' when *x* is a CBS, '*S*' when *x* is a sectionalizer. When SOB *k* differs from SON *i*, firstly the common path is found. When the common path is identical to the whole path of *k* or *i* (that is $s > nm$, in Fig.5) configuration C has to be excluded. Therefore:

- configuration A occurs when the smallest path is the one from PS to the SON (that is $ni < nk$), and then the procedure looks for the CBSs stored in the remaining part of $path_k$; if at least one CBS exists, case 2 occurs and the last CBS is then identified as the opening one; otherwise, case 4 occurs and the opening sectionalizer is the "related switch" of the faulted SOB;
- configuration B occurs when the smallest path is the one from PS to the SOB (that is $ni > nk$), and then the procedure looks for the CBSs stored in the remaining part of $path_i$; if at least one CBS exists, case 3 or 3.1 occurs and the first CBS is then identified as the opening one; otherwise, case 5 occurs and the opening sectionalizer is the first in the remaining part of $path_i$.

Configuration C occurs when the common path is not a fraction of SON or SOB path (that is $s \leq nm$),. Firstly, the procedure looks for the CBSs stored in the remaining part of $path_k$; if at least one CBS exists, case 2 occurs and the last CBS is then identified as the opening one; otherwise the procedure looks for the CBSs stored in the remaining part of $path_i$; if at least one CBS exists, case 3.2 occurs and the first CBS is then identified as the opening one. On the other end, when no CBS is installed in both the remaining paths, case 4 occurs and the sectionalizer installed in SOB *k* is identified as the opening one.

V. Case Study

A. Data input - Segments and cases identification

The reliability indices related to the distribution network in Fig.1 have been assessed by means of the developed software. The failure rate is expressed in terms of faults/year since it is usually computed statistically from historical data. Therefore it is like a failure frequency *f* [32]:

$$f = 8766 \cdot \frac{1}{MTTR + MTTF}$$

where 8766 is the average number of hours in a year accounting for leap years; MTTR and MTTF are the mean time to repair and the mean time to failure, respectively. The mean time between failures (MTBF) is obtained by summing them.

The repair time (t_R) has been assumed equal to the MTTR, thus obtaining that the average number of hours in a year during which the branch is out of service:

$$f \cdot t_r = 8766 \cdot \frac{MTTR}{MTTR + MTTF}$$

Realistic network's data are provided in Tables 3-5 and are referred to the network representation of Fig.1C. In particular, Table 3 reports failure frequency and repair time of each branch, while Table 4 reports the number of customers (N_C) that are connected to each node. Finally, information about the installation branch (*ib*) of each switch, as well as the PoA related to potential islands can be found in Table 5. The table also reports the switching time (t_S) of the sectionalizers installed into the network, and the time to be available (t_{AV}) for the DGs of each island. The data in Tables 1 and 3-5 are the sole inputs for the software, and they are automatically acquired through simple text files [39].

Firstly, the software provides information about SOBs and SONs by using the routines illustrated in Figg.3-4. Table 6 contains the information reported by the software. After that, it applies the fast method to identify the cases. Table 7 reports the cases related to the analyzed network, which have been found by the software. By visual inspection of the network in Fig.1C the exactness of the results is apparent.

TABLE 3
FAILURE RATE AND REPAIR TIME OF THE BRANCHES IN FIG.1C.

ID	f *faults/year*	t_R *hours*
1-6, 36-44	0.05	8.0
7-22, 25-35, 53-56	0.2	6.5
45-52, 57-66	0.25	7.0
23-24	0.3	8.0

TABLE 4
NUMBER OF CUSTOMERS CONNECTED TO THE NODES IN FIG.1C.

ID	N_C
2-3, 5, 40	0
6, 22-24, 31-32, 49-50, 64-66	10
45-48, 57-63	15
9-21, 25-30, 33-35, 51-56	25
1, 4, 7-8, 36-39, 41-44	50

TABLE 5
DATA OF SWITCHES AND RELATED POTENTIAL ISLANDS (FIG.1C).

ID	ib	t_S	PoA	t_{AV}
1	1	-	0.25	0.05
2	5	-	0.25	0.05
3	7	0.15	0.70	0.05
4	17	-	0.30	0.05
5	22	0.15	0.40	0.05
6	23	-	0.60	0.05
7	30	0.15	0.40	0.05
8	40	-	0.25	0.05
9	45	0.1	0.55	0.05
10	51	0.2	0.55	0.05
11	54	0.2	0.60	0.05
12	56	0.2	0.90	0.05

TABLE 6
BRANCHES AND NODES IN FIG.1C, AND RELATED SEGMENTS IN FIG.2.

Segment	branches/nodes
1	1-4, 9-16, 25-27
5	5-6, 28-29, 33-39
7	7-8
17	17-21
22	22, 47-48, 57-58
23	23-24
30	30-32, 49-50
40	40-44, 53
45	45-46
51	51-52, 59-60
54	54-55, 61-66
56	56

TABLE 7
CASES IDENTIFIED BY THE SOFTWARE (FIG.1C).

		SON										
		1	**5**	**7**	**17**	**22**	**23**	**30**	**40**	**45**	**51**	**54**	**56**
	1	1	3	3	3	3	3	3	3	5	3	3	3
	5	2	1	5	2	2	2	5	3	2	3	3	3
	7	2	4	1	2	2	2	4	3.2	2	3.2	3.2	3.2
	17	2	2	2	1	5	3.1	2	2	2	2	2	2
S	**22**	2	2	2	4	1	3	2	2	2	2	2	2
O	**23**	2	2	2	2	2	1	2	2	2	2	2	2
B	**30**	2	4	4	2	2	2	1	3.2	2	3.2	3.2	3.2
	40	2	2	2	2	2	2	2	1	2	5	5	5
	45	4	3.2	3.2	3.2	3.2	3.2	3.2	3.2	1	3.2	3.2	3.2
	51	2	2	2	2	2	2	2	4	2	1	4	4
	54	2	2	2	2	2	2	2	4	2	4	1	4
	56	2	2	2	2	2	2	2	4	2	4	4	1

TABLE 8
TOPOLOGY OF THE NETWORK IN FIG.8. THE LINES ARE IN ASCENDING ORDER.

SN	SB	NB
0	1	28
5	29	3
6	32	7
10	39	8
14	47	8
19	55	7
20	62	3
20	65	1
21	66	1
24	67	1
25	68	1
26	69	1
32	70	5
33	75	3
35	78	2
39	80	3
39	83	2
41	85	3
45	88	1
58	89	1

TABLE 9
FAILURE RATE AND REPAIR TIME OF THE BRANCHES IN FIG.8.

ID	f	t_R
	faults/year	*hours*
1-31	0.02	8.0
32-38, 47-65	0.1	6.0
39-46, 66-77, 80-87	0.2	5.0
78-79, 88-89	0.3	7.0

TABLE 10
NUMBER OF CUSTOMERS CONNECTED TO THE NODES IN FIG.8.

ID	N_C
5, 10, 39, 65	0
62-64, 66-69, 89	10
32-38, 42-61, 75-79, 88	20
1-4, 6-9, 11-28, 40-41, 70-74, 80-87	30
29-31	50

TABLE 11
DATA OF SWITCHES AND RELATED POTENTIAL ISLANDS (FIG.8).

ID	ib	t_S	PoA	t_{AV}
1	1	-	0.10	0.05
2	8	0.15	0.25	0.05
3	15	-	0.60	0.05
4	21	0.10	0.80	0.05
5	29	0.10	0.70	0.05
6	32	-	0.40	0.05
7	39	-	0.50	0.05
8	40	0.15	0.60	0.05
9	42	0.10	0.90	0.05
10	47	0.10	0.50	0.05
11	55	0.10	0.70	0.05
12	70	0.10	0.50	0.05

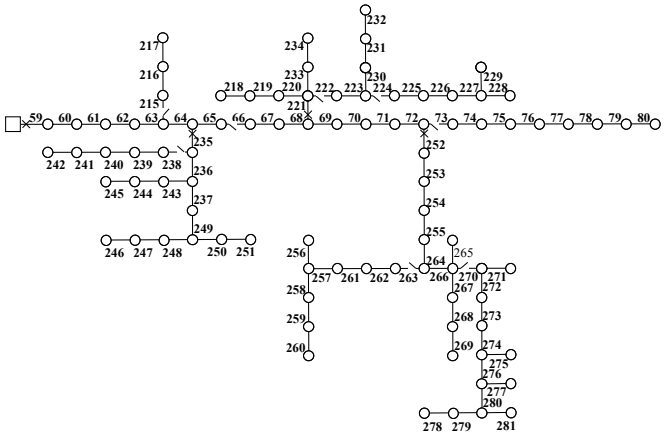

Fig. 6 Real-life EDN in Northwest China.

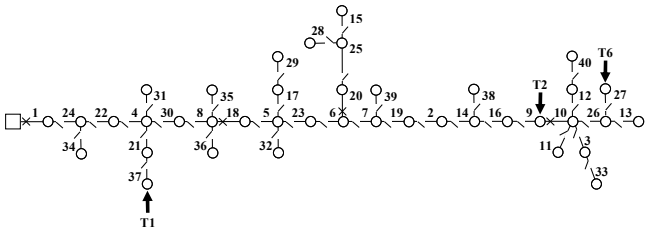

Fig. 7 Modified version of feeder A of network R3-12.47-2 developed by Pacific Northwest National Laboratory, with additional CBSs.

The software has been also applied to a real-life EDN in Northwest China (EDNNC) [54] and to a modified version of R3-12.47-2-Feeder_A (MFA) [55][56] where some CBSs are added. They are depicted, respectively, in Fig.6 and Fig.7. In particular, the network representation reported in Fig.8 and the topology description of Table 8 have been considered for the EDNNC, while Fig.9 refers to the MFA.

Finally, Fig.10 shows the equivalent reduced network obtained by considering segmentation for the EDNNC, while the MFA of Fig.9 in and of itself shows the EDN segments.

Similarly to the previous network, by way of example, realistic input data are reported in Tables 9-11 for the EDNNC.

Segments and cases provided by the software are reported in Tables 12-13. Again, the exactness of the information provided by the software about the segments (reported in Table 12) and the cases (reported in Table 13) can be verified by visual inspection of the network in Figg. 8 and 10.

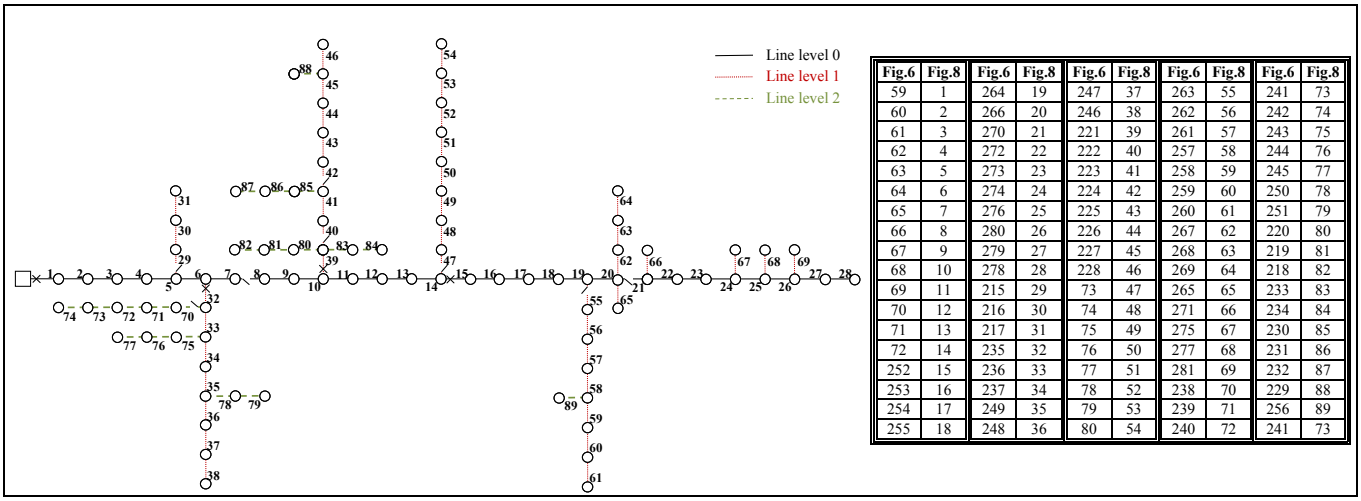

Fig.6	Fig.8	Fig.6	Fig.8	Fig.6	Fig.8	Fig.6	Fig.8	Fig.6	Fig.8
59	1	264	19	247	37	263	55	241	73
60	2	266	20	246	38	262	56	242	74
61	3	270	21	221	39	261	57	243	75
62	4	272	22	222	40	257	58	244	76
63	5	273	23	223	41	258	59	245	77
64	6	274	24	224	42	259	60	250	78
65	7	276	25	225	43	260	61	251	79
66	8	280	26	226	44	267	62	220	80
67	9	279	27	227	45	268	63	219	81
68	10	278	28	228	46	269	64	218	82
69	11	215	29	73	47	265	65	233	83
70	12	216	30	74	48	271	66	234	84
71	13	217	31	75	49	275	67	230	85
72	14	235	32	76	50	277	68	231	86
252	15	236	33	77	51	281	69	232	87
253	16	237	34	78	52	238	70	229	88
254	17	249	35	79	53	239	71	256	89
255	18	248	36	80	54	240	72	241	73

Fig. 8 Equivalent representation of the network in Fig.6.

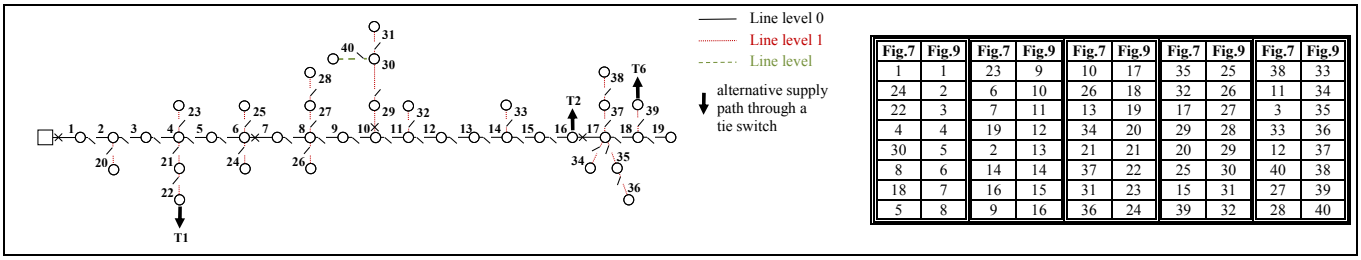

Fig.7	Fig.9	Fig.7	Fig.9	Fig.7	Fig.9	Fig.7	Fig.9	Fig.7	Fig.9
1	1	23	9	10	17	35	25	38	33
24	2	6	10	26	18	32	26	11	34
22	3	7	11	13	19	17	27	3	35
4	4	19	12	34	20	29	28	33	36
30	5	2	13	21	21	20	29	12	37
8	6	14	14	37	22	25	30	40	38
18	7	16	15	31	23	15	31	27	39
5	8	9	16	36	24	39	32	28	40

Fig. 9 Equivalent representation of the network in Fig.7.

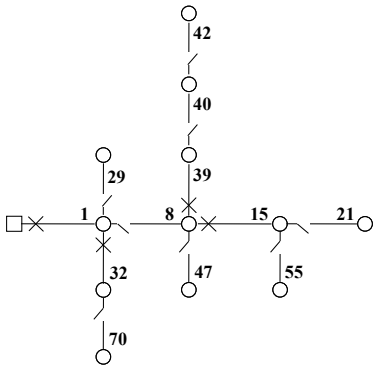

Fig.10 EDNNC's segments.

TABLE 12
BRANCHES AND NODES IN FIG.8, AND RELATED SEGMENTS.

Segments	branches/nodes
1	1-7
8	8-14
15	15-20, 62-65
21	21-28, 66-69
29	29-31
32	32-38, 75-79
39	39, 80-84
40	40-41, 85-87
42	42-46, 88
47	47-54
55	55-61, 89
70	70-74

As for the MFA has been assumed that all the NOSs in the network contain 50 customers; all the SOBs present an equivalent failure frequency and repair time equal to, respectively, 0.02 faults/year and 4 hours.

Four scenarios have been simulated by considering the combination of two sub-scenarios, each one with opposite conditions: (1) manual vs. remote controlled sectionalizers and (2) worst (i.e. PoA=0) vs. best adequacy (i.e. PoA=1). The switching time and the DG time to be available (t_{AV}) have been both set to 1.5h in the scenario considering manual sectionalizers, while they are set to 0.05h for the telecontrolled ones. Worst adequacy means that: the load transfer is never possible by means of tie switches; islanding mode of operation is not permitted by regulation or there is not any DG. On the other hand, best adequacy means that the whole load is always supplied because it is transferred through tie switches

TABLE 13
CASES IDENTIFIED BY THE SOFTWARE FOR THE NETWORK IN FIG.8.

		SON										
		1	**8**	**15**	**21**	**29**	**32**	**39**	**40**	**42**	**47**	**55**	**70**
	1	1	5	3.1	3.1	5	3	3.1	3.1	3.1	5	3.1	3
	8	4	1	3	3	4	3.2	3	3	3	5	3	3.2
	15	2	2	1	5	2	2	2	2	2	2	5	2
	21	2	2	4	1	2	2	2	2	2	2	4	2
S	**29**	4	4	3.2	3.2	1	3.2	3.2	3.2	3.2	4	3.2	3.2
O	**32**	2	2	2	2	2	1	2	2	2	2	2	5
B	**39**	2	2	2	2	2	2	1	5	5	2	2	2
	40	2	2	2	2	2	2	4	1	5	2	2	2
	42	2	2	2	2	2	2	4	4	1	2	2	2
	47	4	4	3.2	3.2	4	3.2	3.2	3.2	3.2	1	3.2	3.2
	55	2	2	4	4	2	2	2	2	2	2	1	2
	70	2	2	2	2	2	4	2	2	2	2	2	1

or the DG is always able to meet the island load or, also, a combination of these conditions occurs.

The input files acquired by the software to perform reliability calculations can be found in [39].

B. *Reliability evaluation and DIgSILENT based validation*

Tables 14 and 15 show the LP reliability indices (i.e. the annual outage rate and duration related to each SON) and some network reliability indices based on them computed by using the analytical formulation described in [33].

In particular, three different scenarios have been investigated. The first scenario assumes that the island mode of operation is permitted in the portions of the network outside from the faulted region, and the values of PoA are reported in Table 5.

Another scenario, which is the worst one, assumes that islanding is not permitted or no DG is installed in the network, that is a PoA equal to 0 for each potential island.

Finally, another scenario, the best one, considers that island mode of operation is always permitted in the portions of the network outside from the faulted region and the DGs of each island are always able to meet the whole local load. The software stores the results about LP and EDN reliability indices in a text file, where it also reports (if requested) some comparisons among the results obtained by using different methods (analytical, RMCS and SMCS). The results reported in the tables and other detailed results are available in [39].

The worst and best scenario have been simulated by DIgSILENT Power Factory to test the exactness of the results. The network simulated in DIgSILENT and the results obtained for the worst scenario are shown in Fig.11. This scenario is equivalent to a condition without DG, thus it has been simulated as explained in the following.

The PS has been emulated by using the "External Grid" component (PS in Fig.11) of DIgSILENT. A "Circuit-Breaker" with a "Probability of Failure" equal to 0% has been considered for each CBS (CBS*x* in Fig.11, where *x* stands for CBS installation branch). A "Disconnector" with a "Probability of Failure" equal to 0% and "Time to actuate the switch" equal to the switching time in Table 5 has been considered for each sectionalizer (S*x* in Fig.11, where *x* stands for the sectionalizer installation branch). A "Line" component of DIgSILENT has been considered to emulate a SOB (B*x* in Fig.11, the other "Line" components, I*x*, are used only for drawing purposes and are set to "Ideal component"). The "Forced Outage Rate" and "Forced Outage Duration" of the "Line" have been set to the values of f and t_R of the SOB, which have been obtained considering the values reported in Table 3. A "General Load" of DPF has been considered to emulate a SON (N*x* in Fig.11). The "Number of connected customers" of the "General Load" has been set to N_c of the SON, which has been obtained considering the values reported in Table 4. All "General Load" components have identical "Load priority". Finally, each "Terminal" component is used only for drawing purpose and it is set to "Ideal component". The "Reliability Assessment - Network connectivity analysis" tool has been adopted for computing LP and system reliability indices. "Automatic Power Restoration" option has been adopted through by using all separation switches. Finally, "Fault Clearance Breakers" has been set to "Use all circuit breakers" while "Switch Actions" has been set to "Parallel".

TABLE 14
LP RELIABILITY INDICES CALCULATED BY THE SOFTWARE (FIG.1C).

	Scenario of Table 5		Worst scenario		Best scenario	
	λ	U	λ	U	λ	U
1	2.90	15.95	2.90	15.95	2.90	15.95
5	4.97	21.09	5.70	25.07	2.80	9.12
7	4.97	17.58	5.70	27.61	2.80	3.02
17	4.23	17.84	5.10	22.63	2.20	6.68
22	4.23	23.44	5.10	30.75	2.20	8.50
23	3.87	23.14	5.70	35.55	0.60	4.80
30	4.97	24.87	5.70	32.31	2.80	7.72
40	7.82	22.73	9.25	28.99	3.55	3.92
45	2.90	10.85	2.90	19.40	2.90	3.86
51	7.82	27.77	9.25	35.79	3.55	7.53
54	7.82	33.53	9.25	41.71	3.55	13.45
56	7.82	21.12	9.25	30.25	3.55	1.99

TABLE 15
SYSTEM RELIABILITY INDICES CALCULATED BY THE SOFTWARE (FIG.1C)

	Scenario of Table 5	Worst scenario	Best scenario
SAIFI	5.1585	5.9313	2.9402
SAIDI	21.0381	25.9527	9.3335
CAIDI	4.0783	4.3756	3.1745

The results in Fig.11 are identical to the ones in Table 14. More specifically, the first value in each "General Load" box is the "Load Point Interruption Frequency" (LPIF) and it is equal to the value of λ in Table 14. The second one in the box is the "Load Point Interruption Time" (LPIT) and it is equal to the value of U in Table 14.

The network simulated in DIgSILENT and the results obtained for the best scenario are shown in Fig.12. This scenario is similar to a condition with DG always able to meet the island's load. This condition has been simulated considering an "External Grid" connected to each leaf of the EDN's topological tree.

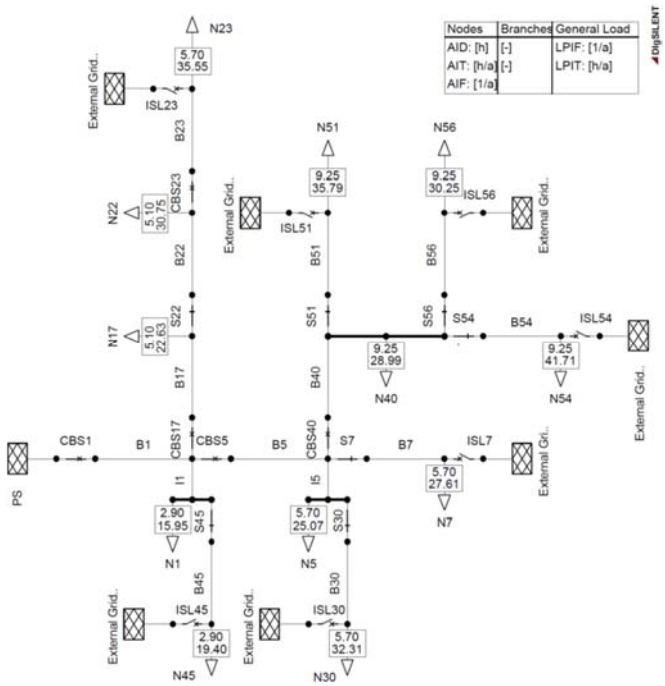

Fig. 11 Outage rate and duration (first and second number in each box) provided by DIgSILENT when the worst scenario is considered for the network in Fig.1C.

Such an approach enables:

- a CBS in the network to trip when an upstream fault occurs, and
- the local load to never be shed whatever the formed island is.

Unfortunately, this approach does not enable to account for the "time to be available", that is t_{AV} in Table 5. This time has to be considered when an island is formed by opening a sectionalizer. More specifically, when the fault is cleared by opening the circuit breaker of a DG too, and a sectionalizer installed between the fault and the DG is subsequently opened the DG can be reconnected. The time to be available of the DG accounts for the time interval between the sectionalizer opening and the DG reconnection. Neglecting this time in DIgSILENT implies that the LPIF of some "General Load" components is slightly less than the value of U in Table 14 for the best scenario. On the other hand, the approach adopted to emulate with DIgSILENT the best scenario does not negatively affect the LPIF of each "General Load", so that it is equal to the value of λ in Table 14.

The LP and system reliability indices provided by the software for the EDNNC are reported, respectively, in Tables 16-17, while the system reliability indices computed for the MFA are in Table 18. More detailed results are available in [39].

Similarly to the previous network, the DIgSILENT software has been used to prove the exactness of the results when the option of operating some parts of the network in island mode: is neglected (worst scenario); is not neglected and the DGs in each island always meet the local load (best scenario). Moreover, for the MFA two sub-scenarios have been considered: manual and telecontrolled sectionalizers.

Figg. 13-14 show the results obtained for the EDNNC, while the Figg.15-18 show the results obtained for the MFA. The comparison of the results obtained with DIgSILENT and the proposed software confirms the previous considerations.

TABLE 16
LP RELIABILITY INDICES PROVIDED BY THE SOFTWARE (FIG.8).

	Scenario of Table 13		Worst scenario		Best scenario	
	λ	U	λ	U	λ	U
1	1.14	1.23	1.14	1.23	1.14	1.23
8	1.14	2.05	1.14	2.33	1.14	1.23
15	3.00	4.87	3.62	5.88	2.48	3.56
21	3.00	7.43	3.62	11.07	2.48	5.46
29	1.14	0.93	1.14	1.70	1.14	0.60
32	3.58	12.24	4.04	12.73	2.90	11.50
39	4.12	7.72	4.64	8.61	3.50	6.28
40	4.12	9.11	4.64	13.46	3.50	5.37
42	4.12	11.71	4.64	20.43	3.50	7.49
47	1.14	6.22	1.14	7.05	1.14	4.85
55	3.00	8.77	3.62	12.08	2.48	6.47
70	3.58	11.58	4.04	17.63	2.90	5.28

TABLE 17
SYSTEM RELIABILITY INDICES PROVIDED BY THE SOFTWARE (FIG.8).

	Scenario of Table 13	Worst scenario	Best scenario
SAIFI	2.7417	3.1156	2.3358
SAIDI	6.9560	9.2580	5.0732
CAIDI	2.5371	2.9715	2.1719

TABLE 18
SYSTEM RELIABILITY INDICES PROVIDED BY THE SOFTWARE (FIG.9).

	Worst scenario		Best scenario	
	Manual	Telecontrolled	Manual	Telecontrolled
SAIFI	0.4985	0.4985	0.233	0.233
SAIDI	1.2952	0.8900	0.4925	0.0937
CAIDI	2.5983	1.7853	2.1137	0.4024

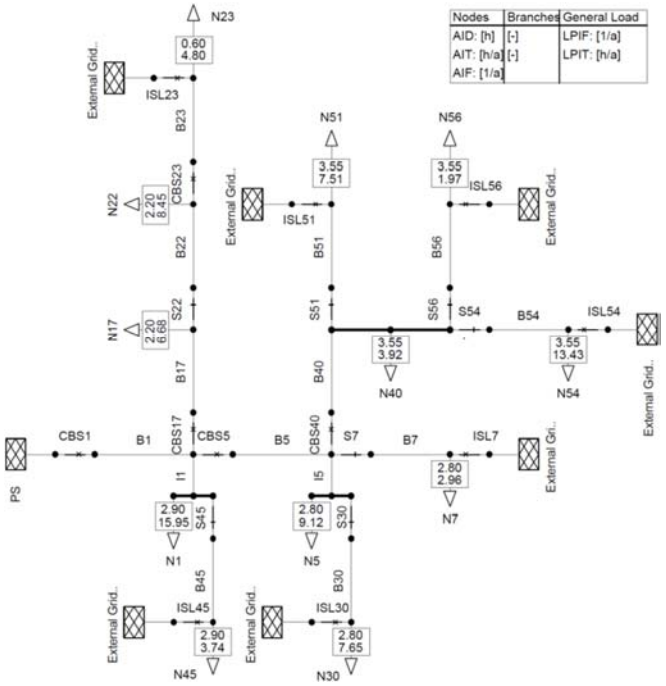

Fig. 12 Outage rate and duration provided by DIgSILENT when the best scenario is considered for the network in Fig.1C.

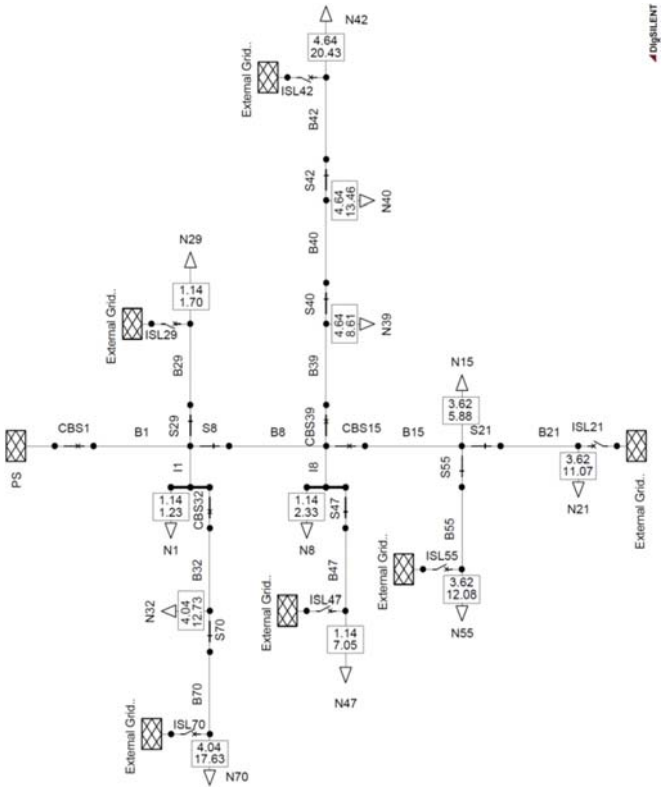

Fig. 13 Outage rate and duration provided by DIgSILENT when the worst scenario is considered for the EDNNC (Figg.8 and 10).

Fig. 14 Outage rate and duration provided by DIgSILENT when the best scenario is considered for the EDNNC (Figg.8 and 10).

VI. Conclusions

The main procedures of a software able to assess distribution reliability indices accounting for islanding has been proposed. A simple and efficient network representation and data structure exploited by these procedures to perform more quickly their tasks is described. More specifically, a procedure stores some network topological information that enables a faster execution of the other one. The information is obtained without any further computational effort thanks to the proposed network representation and data structure.

The software has been applied to a test system and two real-life networks. It has been shown that simple information has to be provided as input in order to compute the reliability indices of radial distribution networks accounting for autonomous microgrids. The code ability to correctly identify SOBs, SONs and topological cases has been verified. Moreover, the worst and the best scenario have been simulated with DIgSILENT Power Factory to validate the results.

The code of the developed software is available online under the GNU General Public License. Therefore, researchers and practitioners can use the code or modify it in order to implement their methods or to improve the results accuracy. Moreover, further research could focus on overcoming potential limitations of the implemented analytical and MCS methods, on integrating new features in the system analysis, on combining the software with optimization methods, and so on.

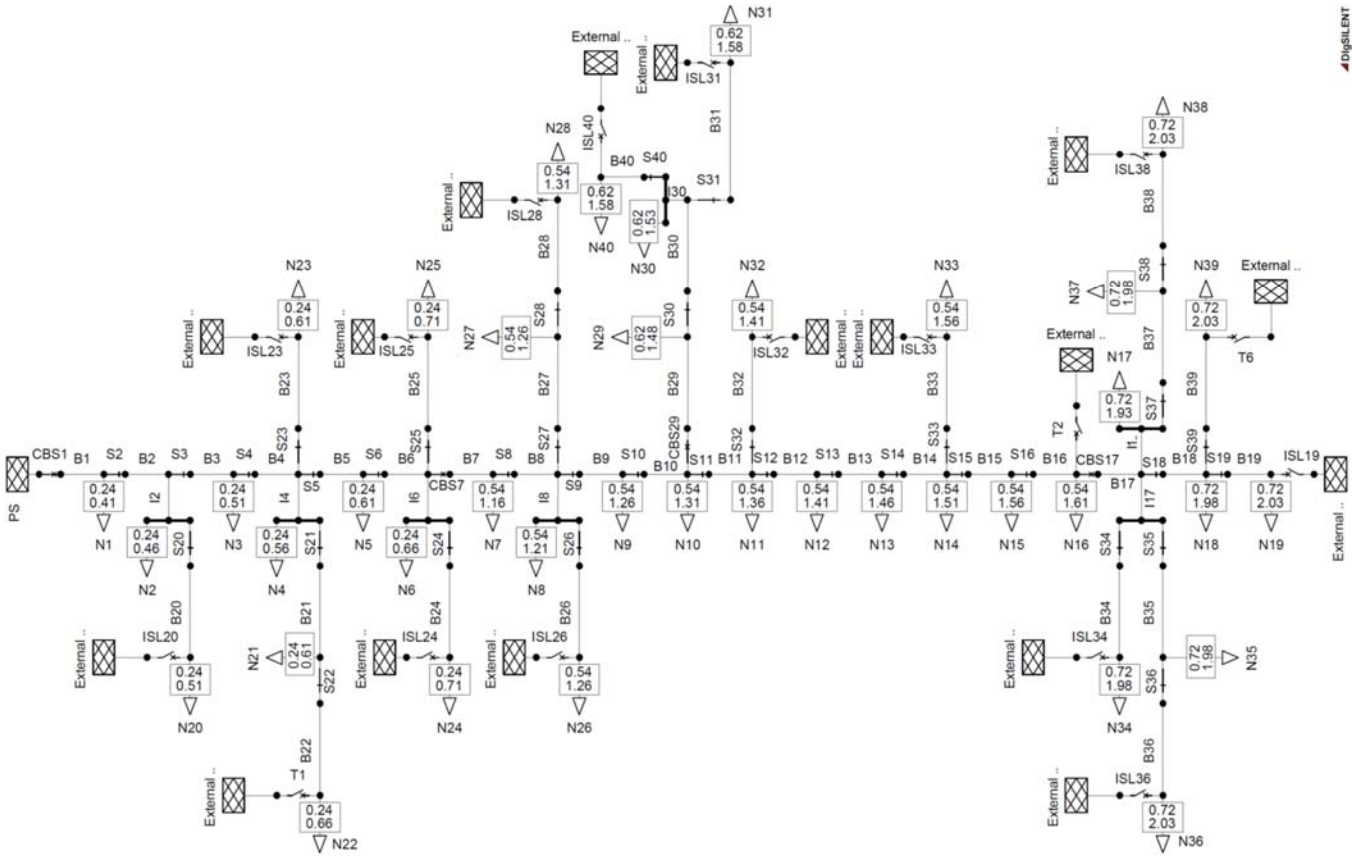

Fig. 15 Outage rate and duration provided by DIgSILENT when the worst scenario and manual sectionalizers are considered for the MFA (Fig. 9).

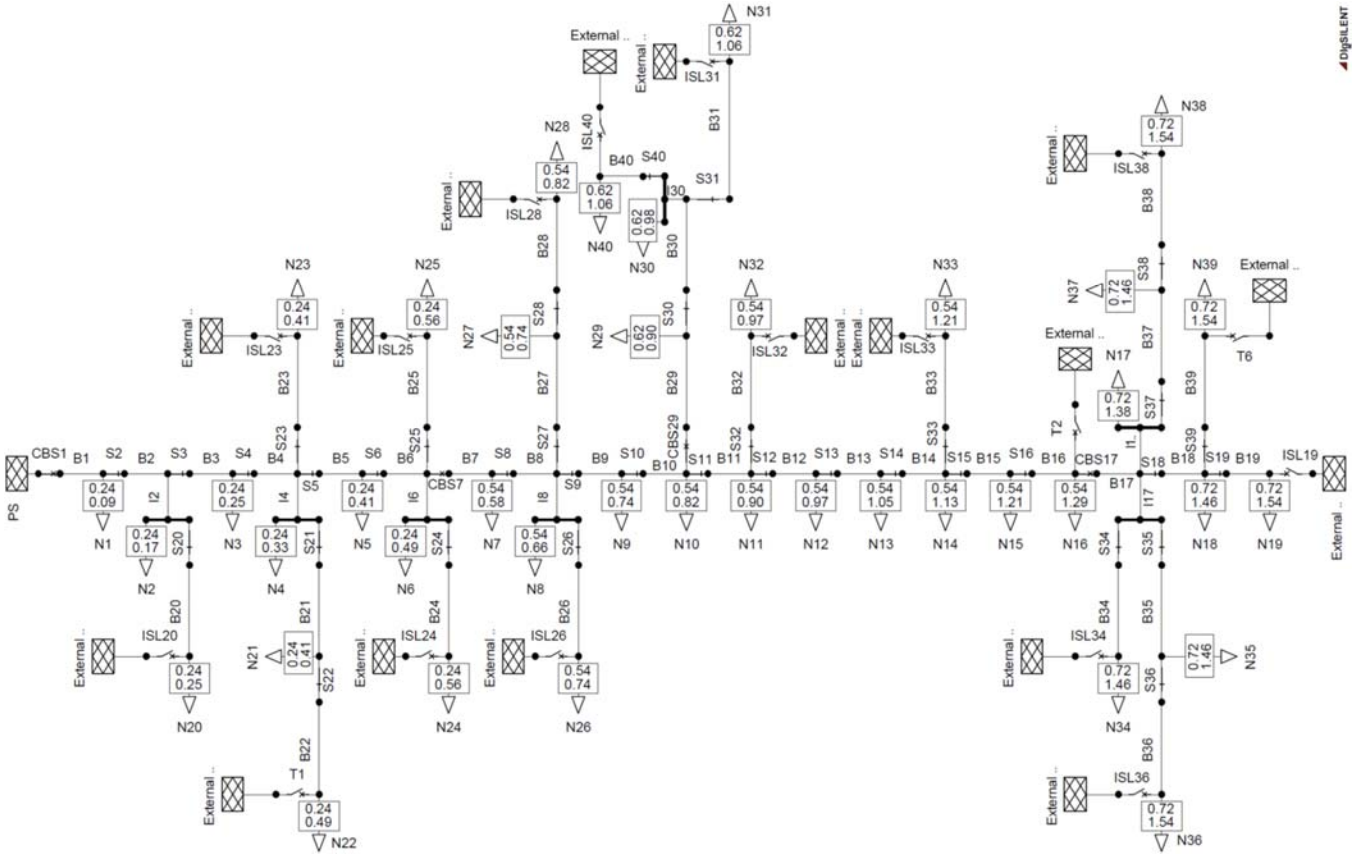

Fig. 16 Outage rate and duration provided by DIgSILENT when the worst scenario and telecontrolled sectionalizers are considered for the MFA (Fig.9).

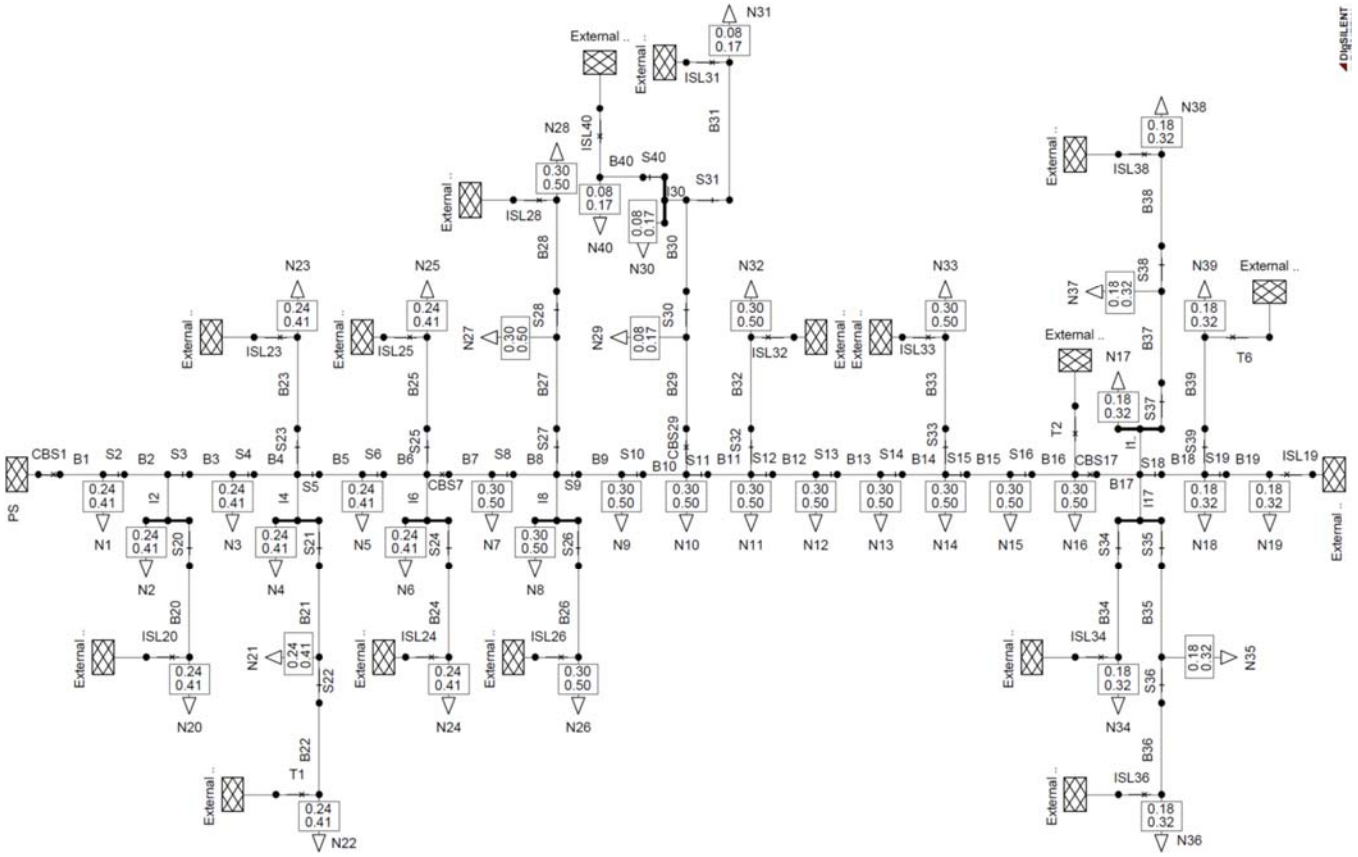

Fig. 17 Outage rate and duration provided by DIgSILENT when the best scenario and manual sectionalizers are considered for the MFA (Fig.9).

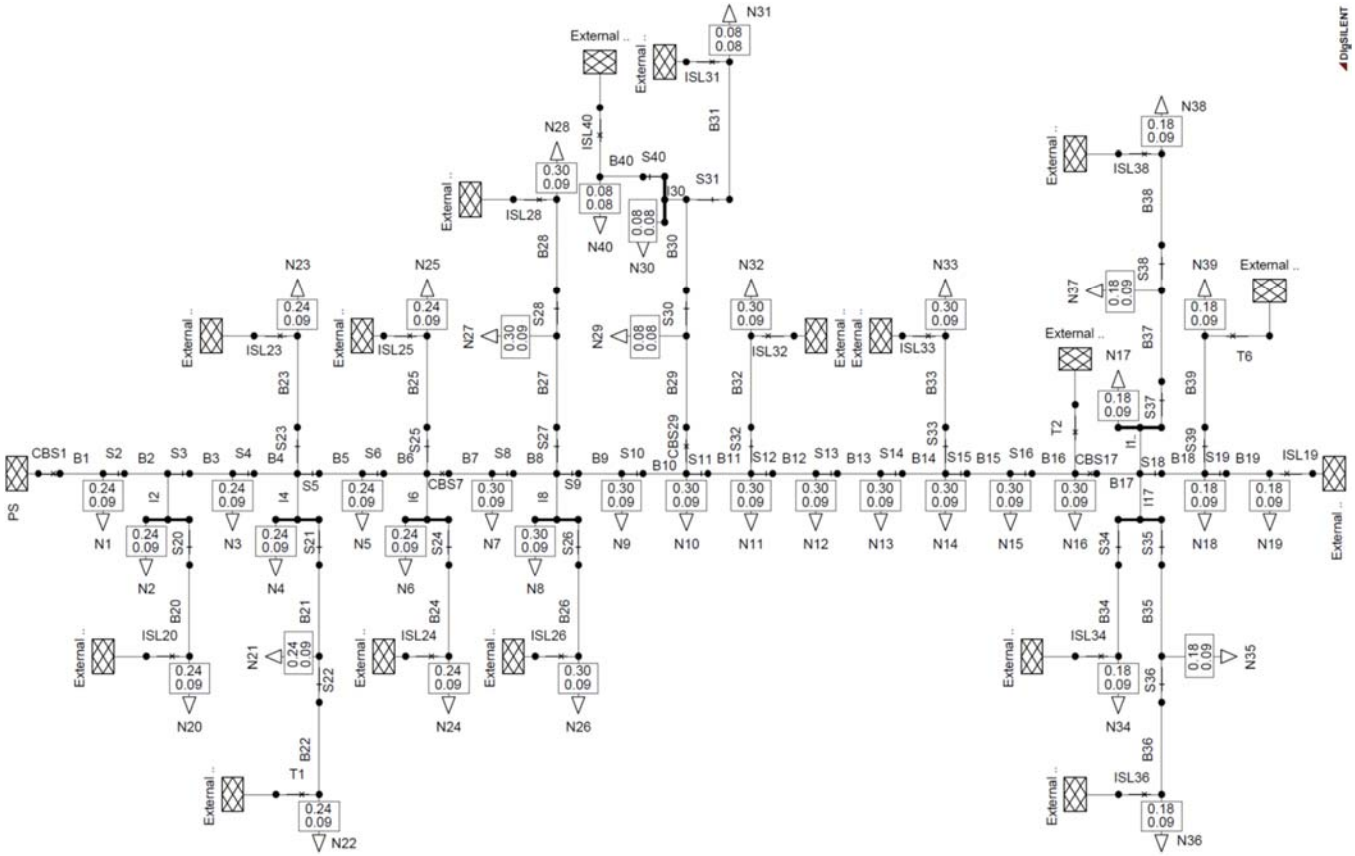

Fig. 18 Outage rate and duration provided by DIgSILENT when the best scenario and telecontrolled sectionalizers are considered for the MFA (Fig.9).

REFERENCES

[1] Billinton, R., Wang, P.: Distribution system reliability cost/worth analysis using analytical and sequential simulation techniques. IEEE Trans. on Power Systems, 13, 1245-1250 (1998).

[2] Tippachon, W., Rerkpreedapong, D.: Multiobjective optimal placement of switches and protective devices in electric power distribution systems using ant colony optimization. Electric Power Systems Research, 79, 1171-1178 (2009).

[3] Ferreira, D., Bretas, A.S.: A nonlinear binary programming model for electric distribution systems reliability optimization. International Journal of Electrical Power & Energy Systems, 43, 384-392 (2012).

[4] Siirto, O., Hyvärinen, M., Loukkalahti, M., Hämäläinen, A., Lehtonen, M.: Improving reliability in an urban network. Electric Power Systems Research, 120, 47-55 (2015).

[5] Barabadi, A., Aliyari, M.: Maintenance Planning for Electricity Distribution Networks Using Reliability Indices. International Review of Electrical Engineering, 10, 646-652 (2015).

[6] Ray, S., Bhattacharya, A., Bhattacharjee, S.: Optimal placement of switches in a radial distribution network for reliability improvement. International Journal of Electrical Power & Energy Systems, 76, 53-68 (2016).

[7] López, J.C., Lavorato, M., Rider, M.J.: Optimal reconfiguration of electrical distribution systems considering reliability indices improvement. International Journal of Electrical Power & Energy Systems, 78, 837-845 (2016).

[8] Popović, Ž., Brbaklić, B., Knežević, S.: A mixed integer linear programming based approach for optimal placement of different types of automation devices in distribution networks. Electric Power Systems Research, 148, 136-146 (2017).

[9] Rodríguez-Calvo, A., Cossent, R., Frías P.: Assessing the potential of MV automation for distribution network reliability improvement. Int. Trans. Electr. Energ. Syst. (2017). doi:10.1002/etep.2383.

[10] Balijepalli, N., Venkata, S.S., Christie, R.D.: Predicting distribution system performance against regulatory reliability standards. IEEE Transactions on Power Delivery, 19, 350-356.(2004).

[11] Assis, T.M.L., Taranto, G.N., Falcão, D.M., Ferreira, P.M.B., Pontes, C.E.V., Mendonça, L.P.: Pilot field test of intentional islanding in distribution network". Energy Systems (2015). doi:10.1007/s12667-015-0159-3

[12] Allan, R.N., Billinton, R., De Oliveira, M.F.: An Efficient Algorithm for Deducing the Minimal Cuts and Reliability Indices of a General Network Configuration. IEEE Transactions on Reliability, R-25, 226-233 (1976).

[13] Kjolle, G., Sand, K.: RELRAD-an analytical approach for distribution system reliability assessment. IEEE Transactions on Power Delivery, 7, 809-814 (1992).

[14] Billinton, R., Zhang, W.: Algorithm for failure frequency and duration assessment of composite power systems. IEE Proceedings Generation, Transmission and Distribution, 145, 117 - 122 (1998).

[15] Billinton, R., Wang, P. Reliability-network-equivalent approach to distribution-system-reliability evaluation. IEE Proceedings Generation, Transmission and Distribution, 145, 149-153 (1998).

[16] Koval, D.O.: Zone-branch reliability methodology for analyzing industrial power systems. IEEE Transactions on Industry Applications, 36,.1212-1218 (2000).

[17] Xie, K., Zhou, J., Billinton, R.: Reliability evaluation algorithm for complex medium voltage electrical distribution networks based on the shortest path. IEE Proceedings Generation, Transmission and Distribution, 150, 686-690, (2003).

[18] Xie, K., Zhou, J., Billinton, R.: Fast algorithm for the reliability evaluation of large-scale electrical distribution networks using the section technique. IET Proceedings Generation, Transmission & Distribution, 2, 701-707 (2008).

[19] Liu, Y., Singh, C.: Reliability Evaluation of Composite Power Systems Using Markov Cut-Set Method. IEEE Transactions on Power Systems, 25, 777-785 (2010).

[20] Ekonomou, L., Fotis, G.P., Vita, V., Mladenov, V.: Distributed Generation Islanding Effect on Distribution Networks and End User Loads Using the Master-Slave Islanding Method. Journal of Power and Energy Engineering, 4, 1-24 (2016)

[21] Heidari, A., Agelidis, V.G., Zayandehroodi, H., Pou, J., Aghaei, J.: On Exploring Potential Reliability Gains Under Islanding Operation of Distributed Generation. IEEE Transactions on Smart Grid, 7, 2166-2174 (2016).

[22] Kreishan, M.Z., Fotis, G.P., Vita, V., Ekonomou, L., Distributed Generation Islanding Effect on Distribution Networks and End User Loads Using the Load Sharing Islanding Method. Energies (2016). doi:10.3390/en9110956.

[23] Bie, Z., Zhang, P., Li, G., Hua, B., Meehan, M., Wang, X.: Reliability Evaluation of Active Distribution Systems Including Microgrids. IEEE Trans. on Power Systems, 27, 2342-2350 (2012).

[24] Ge, S., Xu, L., Liu, H., Zhao, M.: Reliability Assessment of Active Distribution System Using Monte Carlo Simulation Method. Journal of Applied Mathematics (2014) doi:10.1155/2014/421347.

[25] Li, G., Bie, Z., Xie, H., Lin, Y.: Customer satisfaction based reliability evaluation of active distribution networks. Applied Energy, 162, 1571-1578 (2016).

[26] Araújo, J.R., Silva, E.N.M., Rodrigues, A.B., da Silva, M.G.: Assessment of the Impact of Microgrid Control Strategies in the Power Distribution Reliability Indices. Journal of Control, Automation and Electrical Systems, 28, 271–283 (2017).

[27] Hashemi-Dezaki, H., Askarian-Abyaneh, H., Shams-Ansari, A., DehghaniSanij, M., Hejazi, M.A.: Direct cyber-power interdependencies-based reliability evaluation of smart grids including wind/solar/diesel distributed generations and

plug-in hybrid electrical vehicles. International Journal of Electrical Power & Energy Systems, 93, 1-14 (2017).
[28] Moeini-Aghtaie, M., Farzin, H., Fotuhi-Firuzabad, M., Amrollahi, R.: Generalized Analytical Approach to Assess Reliability of Renewable-Based Energy Hubs. IEEE Transactions on Power Systems, 32, 368-377 (2017).
[29] Al-Muhaini, M., Heydt, G.T.: Evaluating Future Power Distribution System Reliability Including Distributed Generation. IEEE Transactions on Power Delivery, 28, 2264-2272 (2013).
[30] Chen, Y., Zheng, Luo, Y.F., Wen, J., Xu, Z.: Reliability evaluation of distribution systems with mobile energy storage systems, IET Renew. Power Gener., 10, 1562-1569 (2016).
[31] Chen, C., Wu, W., Zhang, B., and Singh, C.: An Analytical Adequacy Evaluation Method for Distribution Networks Considering Protection Strategies and Distributed Generators, IEEE Transactions on Power Delivery, 30, 1392-1400 (2015).
[32] Conti, S., Rizzo, S.A.: Monte Carlo Simulation by using a Systematic Approach to Assess Distribution System Reliability considering Intentional Islanding. IEEE Transactions on Power Delivery, 30, 64-73 **(**2015).
[33] Conti, S., Nicolosi, R., Rizzo, S.A.: Generalized Systematic Approach to Assess Distribution System Reliability with Renewable Distributed Generators and Micro-Grids. IEEE Transactions on Power Delivery, 27, 1, 261-270 (2012).
[34] Anderson, K., Du, J., Narayan, A., El Gamal, A.: GridSpice: A Distributed Simulation Platform for the Smart Grid. IEEE Transactions on Industrial Informatics,10, 2354-2363, 2014.
[35] Sijakovic, N., Djuric, M., Kostic, M., Ekonomou, L.: An open source tool for transmission system analysis and planning. Energy Systems (2014) doi:10.1007/s12667-014-0125-5.
[36] Lazarou, S., Oikonomou, D.S., Ekonomou, L.: A platform for planning and evaluating distributed generation connected to the Hellenic electric distribution grid. 11th WSEAS Int. Conf. on Circuits, Systems, Electronics, Control and Signal Processing (CSECS'12), Montreux, Switzerland, pp. 80-86, 2012.
[37] Lazarou, S. Vita, V., Karampelas, P., Ekonomou, L.:A power system simulation platform for planning and evaluating distributed generation systems based on GIS. Energy Systems (2013) doi:10.1007/s12667-013-0082-4.
[38] Morante, Q., Ranaldo, N., Vaccaro, A., Zimeo, E.: Pervasive grid for large-scale power systems contingency analysis. IEEE Transactions on Industrial Informatics, 2, 165-175 (2006).
[39] http://www.dieei.unict.it/users/sconti/psrs.htm
[40] Allam, M.A., Hamad, A.A., Kazerani, M., El-Saadany, E.F.: A steady-state analysis tool for unbalanced islanded hybrid AC/DC microgrids. Electric Power Systems Research, 152, 71-83 (2017).
[41] Shotorbani, A.M., Ghassem-Zadeh, S., Mohammadi-Ivatloo, B., Hosseini, S.H.: A distributed secondary scheme with terminal sliding mode controller for energy storages in an islanded microgrid. International Journal of Electrical Power & Energy Systems, 93, 352-364 (2017).
[42] Mokryani, G., Hu, Y.F., Papadopoulos, P., Niknam, T., Aghaei, J.: Deterministic approach for active distribution networks planning with high penetration of wind and solar power. Renewable Energy, 113, 942-951 (2017).
[43] Hosseinnezhad, V., Rafiee, M., Ahmadian, M., Siano, P.: Optimal day-ahead operational planning of microgrids. Energy Conversion and Management. 126, 142-157 (2016).
[44] Hutterer, S., Beham, A., Affenzeller, M., Auinger, F., Wagner, S.: Software-Enabled Investigation in Metaheuristic Power Grid Optimization. IEEE Transactions on Industrial Informatics, 10, 364-372 (2014).
[45] Zhang, Y., Gatsis, N., Giannakis, G.B.: Robust Energy Management for Microgrids With High-Penetration Renewables. IEEE Sustainable Energy, 4, 944-953 (2013).
[46] Arefifar, S.A., Mohamed, Y.A.R.I., El-Fouly, T.H.M.: Supply-Adequacy-Based Optimal Construction of Microgrids in Smart Distribution Systems. IEEE Transactions on Smart Grid, 3, 1491-1502 (2012).
[47] Wang, P., Gao Z., Bertling, L.: Operational Adequacy Studies of Power Systems With Wind Farms and Energy Storages. IEEE Transactions on Power Systems, 27, 4, 2377-2384 (2012).
[48] Olivares, D.E., Cañizares, C.A., Kazerani, M. A Centralized Energy Management System for Isolated Microgrids. IEEE Transactions on Smart Grid, 5, 1864-1875 (2014).
[49] Wang, C., Jiao, B., Guo, L., Yuan, K., Sun, B.: Optimal planning of stand-alone microgrids incorporating reliability. Journal of Modern Power Systems and Clean Energy, 2, 195–205 (2014).
[50] Koh, L.H., Wang, P., Choo, F.H., Tseng, K.J., Gao, Z., Püttgen, H.B.: Operational Adequacy Studies of a PV-Based and Energy Storage Stand-Alone Microgrid. in IEEE Transactions on Power Systems, 30, 892-900 (2015).
[51] Parhizi, S., Lotfi, H., Khodaei, A., Bahramirad, S.: State of the Art in Research on Microgrids: A Review. IEEE Access, 3, 890-925 (2015).
[52] Conti, S., Faraci, G., La Corte, A., Nicolosi, R., Rizzo, S.A., Schembra, G.: Effect of Islanding and Telecontrolled switches on Distribution System Reliability Considering Load and Green-Energy Fluctuations. Applied Sciences (2016). doi:10.3390/app6050138.
[53] Conti, S., Rizzo, S.A.: Probability of Adequacy Evaluation Considering Power Output Correlation of Renewable Generators in Smart Grids. *I*nternational Journal of Electrical Power & Energy Systems, 61, 145-151 (2014.
[54] Bie, Z., Zhang, P., Li, G., Hua, B., Meehan, M., Wang, X.: Reliability Evaluation of Active Distribution Systems Including Microgrids. IEEE Trans. on Power Systems, 27, 2342-2350 (2012).
[55] Li, J., Ma, X.Y., Liu, C.C., Schneider, K.P.: Distribution System Restoration With Microgrids Using Spanning Tree Search. IEEE Transactions on Power Systems, 29, 3021-3029 (2014).
[56] Jiang, Y., Liu, C.C., Xu, Y.: Smart Distribution Systems. Energies (2016). doi:10.3390/en9040297